HHS Public Access

Author manuscript

Cancer Res. Author manuscript; available in PMC 2018 January 15.

Published in final edited form as:

Cancer Res. 2017 January 15; 77(2): 448–458. doi:10.1158/0008-5472.CAN-16-2350.

Chemopreventive effects of ROS targeting in a murine model of BRCA1-deficient breast cancer

Mo Li[1,2], **Qian Chen**[2], and **Xiaochun Yu**[2,*]

[1]Center of Reproductive Medicine, Department of Obstetrics and Gynecology, Peking University Third Hospital, Beijing, China

[2]Department of Cancer Genetics and Epigenetics, Beckman Research Institute, City of Hope, Duarte, CA 91010, USA

Abstract

There remains great interest in practical strategies to limit the elevated risks of familial breast and ovarian cancers driven by BRCA1 mutation. Here we report that limiting the production of reactive oxygen species (ROS) is sufficient to reduce DNA lesions and delay tumorigenesis in a murine model of BRCA1-deficient breast cancer. We documented a large amount of endogenous estrogen oxidative metabolites in the mammary gland of the model, which induced DNA adducts and apurinic/apyrimidinic sites associated with DNA double-strand breaks and genomic instability. Repressing estrogen oxidation via antioxidant treatments reduced oxidative DNA lesions and delayed the onset of mammary tumors. Overall our work suggests an answer to the long-standing question of why germline BRCA1 mutations cause tissue-specific tumors, in showing how tissue-specific, ROS-induced DNA lesions create a non-genetic force to promote mammary tumors in BRCA1-deficient mice. Our findings create a rationale for evaluating suitable antioxidant modalities as a chemopreventive strategy for familial breast cancer.

Keywords

DNA damage response; DNA damage repair; BRCA1; ROS; breast cancer

Introduction

Women with germline *BRCA1* mutations have lifetime threat to develop breast and ovarian cancers (1,2). Also, loss of the *BRCA1* gene expression by promoter hypermethylation contributes to sporadic breast and ovarian cancers (3), suggesting that BRCA1 plays an important role in breast and ovarian tumor suppression.

Accumulated evidence suggests that BRCA1 is involved in DNA damage response and maintaining genomic stability under genotoxic stress (4). In response to DNA double-strand breaks (DSBs), BRCA1 is phosphorylated by a group of PI3 kinases including ATM, ATR and DNA-PK, and acts as a mediator to regulate downstream CHK1 kinase activity, which

*Corresponding author: Phone: (626)218-5724; FAX: (626)218-0403; xyu@coh.org.

Conflict of Interest: The authors declare no potential of conflict of interest.

controls DSB-induced cell cycle checkpoint activation (5–7). Lacking BRCA1 impairs DSB-induced checkpoint activation. Thus, DNA damage repair machinery does not have enough time to repair DNA lesions. If not repaired, these lesions could be duplicated during DNA replication in S phase and transmitted from mother cells to daughter cells during mitosis, which induces genomic instability (8). Moreover, BRCA1 is associated with several key effectors, such as RAD51, PALB2 and BRCA2, during homologous recombination (HR), a high fidelity type of repair for DSBs (9,10). Thus, loss of BRCA1 disrupts HR and induces genomic instability (11).

In mammals, BRCA1 is essential for cell growth. Thus, human cancer-associated *BRCA1* mutations are either hypomorphic mutations or associated with other genetic alterations, such as *p53* mutations, to facilitate oncogenic growth (12). Based on cancer genetic analyses, several groups have established mammary gland tumor models in tissue-specific BRCA1-deficient mice to recapitulate human breast tumorigenesis (13). In particular, conditional deletion of *Brca1* in the mammary gland using *β-lactoglobin (Blg)-Cre* in the heterozygous mutation of *p53* background results in high histological grade mammary tumor with strong resemblance of human BRCA1-related breast tumor. Thus, these genetic studies clearly demonstrate that BRCA1 deficiency is a genetic driving force to induce breast cancer. However, it is still unclear why BRCA1 mutation carriers are only predisposed to breast and ovarian tumors.

Since BRCA1 is evolutionarily conserved in most eukaryotes, lacking BRCA1 should induce genomic instability in most cells. As BRCA1 mutations mainly cause breast and ovarian tumorigenesis, we hypothesize that tissue-specific mutagens may exist in breast and ovarian tissues and induce cell transformation in the absence of BRCA1. One candidate of tissue-specific carcinogen is estrogen as it is remarkably enriched in both breast tissue and ovary from puberty to pregnancy (14). Estrogen itself is a female sex hormone for the development of mammary gland and female reproduction system. However, during estrogen metabolism, it can be oxidized into quinone radicals that induce oxidative damage on genomic DNA (15), which may require BRCA1-dependent pathway to repair the lesions(16). Epidemiology study also reveals that excessive exposure to estrogen associates with higher risk to breast cancer (17). Thus, oxidative metabolites of estrogen may be the potential driver for BRCA1-related breast cancer.

To study the molecular mechanism by which BRCA1 deficiency induces breast cancer, we characterized a mouse mammary tumor model with specifically knocking out *Brca1* in mammary gland. We found that endogenous estrogen metabolites induce oxidative damage that leads to DSBs. Without BRCA1, cells could not repair DSBs, which results in genomic instability and tumorigenesis. Antioxidant treatment suppresses estrogen metabolites-induced DNA lesions, and significantly delays the onset of Brca1 deficiency-induced tumorigenesis. Thus, repression of estrogen oxidative metabolism could be a potential strategy for the eradication of familial breast cancer.

Materials and Methods

Chemical, antibodies and cells

All the chemicals were purchased from Sigma except for those specifically mentioned. Anti-γH2AX antibody was purchased from Cell Signaling Technology; Anti-53BP1 and Rad51 antibodies were purchased from Novus Biologicals. HCC1937 cells were obtained from ATCC in 2008, HCC1937 cells reconstituted with wild-type BRCA1 (HCC1937 BRCA1 cells) were generated in our lab in 2008.

Animal strains and maintenance

Blg-cre mice were purchased from Jackson Laboratory. *BRCA1*$^{flox/+}$ mice were kindly gifted from Dr. Kathleen Cho at University of Michigan. Cre recombinase removes exon 5–13 of *Brca1*. *p53*$^{flox/+}$ mice were kindly gifted from Professor Yuan Zhu at University of Michigan (currently at Children's National Medical Center in Washington D.C.). Cre recombinase removes exon 2–10 of *p53*. The *Brca1*$^{flox/+}$ mice were intercrossed with *p53*$^{flox/+}$ mice to create the *Brca1*$^{flox/+}$; *p53*$^{flox/+}$ mice. The *BRCA1/p53* floxed mice were further crossed with the *Blg-Cre* transgenic mice to generate *Blg-Cre*; *Brca2*$^{flox/flox}$; *p53*$^{flox/+}$ mice (BBP mice). The *Blg-Cre*; *Brca1*$^{+/+}$; *p53*$^{+/+}$ mice were used for the WT counterparts. All parallel experiments were performed by using the littermate mice from a mixed but uniform genetic background. Female mice mated from 10 weeks. The animals were maintained in a specific pathogen-free environment under a 12 hour light/dark cycle. Mice were euthanized by CO_2 when the main breast tumor grew to no more than 2.5 cm in diameter. All experiments were performed in accordance with national and institutional guidelines. The animal protocol of this study was approved by the ethical review committee of the University of Michigan (UCUCA PRO00005209).

Genotyping

DNA was isolated from mouse tails using the DAeasy Blood and Tissue Kit (Qiagen, Valencia, CA) and genotyped by PCR. Reaction conditions for *Cre*, *Brca1,* and *p53* were 40 cycles of 94 °C for 30 seconds, 60 °C for 30 seconds, and 72 °C for 1 minute. PCR products were examined in the 1.5 % agarose gel.

Histology and immunofluorescence

Explanted tissues were fixed in 10 % neutral-buffered formalin solution for at least 16 hours and gradually transferred to 70 % ethanol. Then the tissues were embedded in paraffin at University of Michigan Microscopy & Image Analysis Core, cut in 5μm sections on poly-lysine coated slides, deparaffinized, rehydrated, and stained with hematoxylin and eosin (H&E). Images were taken by an Olympus IX 71 microscope with the CellSens software. For tissue immunofluorescence staining, after deparaffinization and rehydration, sections were unmasked in 10 mM citric acid (pH 6.0) in a microwave for 20 minutes. Then the samples were subjected to standard immunofluorescence staining. Briefly, tissues were incubated in primary antibody overnight at 4 °C. After washed in PBS three times, the samples were incubated in FITC-conjugated or Rho-conjugated IgG for 1 hour at room temperature. After washing and staining by Hoechst 33342, tissues were mounted in anti-

fade and observed under the Olympus IX 71 microscope with the CellSens software. Regarding immunofluorescence of cells, cells were fixed in 3% paraformaldehyde for 25 minutes and permeabilized in 0.5 % Triton X-100 for 20 minutes at room temperature. Samples were blocked with 5 % goat serum and then incubated in primary antibody for 60 minutes. After that, sections were washed with PBS three times and incubated with fluorescent secondary antibody for 40 minutes. Following PBS wash, the nuclei were stained by Hoechst 33342. The signals were visualized by the fluorescence microscope and analyzed by CellSens software.

AP sites assay

After standard deparaffinization, rehydration, and unmasking described above, sections were stained for the AP sites using DNA damage - AP site assay kit (abcam, ab133076) according to the provided protocol for “Fluorescence Microscopy”. AP sites in the tissues were labeled by Avidin-FITC and detected by the Olympus IX 71 microscope (excitation/emission = 485/535).

Synthesis of 4-OHE_2-1-N3Ade and 4-OHE_2-1-N7Gua

The synthesis of depurinating DNA adducts 4-OHE_2-1-N3Ade and 4-OHE2-1-N7Gua was performed according to the reported procedure (17). Briefly, to a suspension of activated MnO_2 (119 mg, 1.37 mmol) in 5 ml of dimethylformamide (DMF) at 0 °C was added 4-OHE_2 (60 mg, 0.21 mmol). After 10 min of stirring at 0 °C, the resulting E_2-3,4-Q in DMF was filtered, directly added dropwise into a stirred solution of Ade (1.26 mmol) dissolved in 5 ml of acetic acid and water (1:1, v/v), and allowed to react for 5 hours with stirring at room temperature. The solution was then filtered and purified by HPLC. The yield of 4-OHE_2-1-N3Ade was around 57 %. For 4-OHE_2-1-N7Gua, a suspension of 4-OHE_2 (0.18 mmol) in 5 ml of acetonitrile (CH_3CN) was cooled to 0 °C prior to the addition of activated MnO_2 (1.18 mmol). The suspension was stirred for 10 minutes and then filtered directly into a stirred solution of dG (0.94 mmol) dissolved in 10 ml of acetic acid and water (1:1, v/v), allowing to react for 5 hours with stirring at room temperature. The solution was then filtered and purified by HPLC. The yield of 4-OHE_2-1-N7Gua was around 40%.

Detection of depurinating DNA adducts

Extraction of depurinating DNA adducts was performed according to the previous study with minor revision. Briefly, approximately 1 g of ground mammary tissue was suspended in 3 ml of 1 % acetic acid and incubated 5 hours at room temperature. Afterwards, the depurinating DNA adducts, 4-OHE_2-1-N3Ade and 4-OHE_2-1-N7Gua, were Soxhlet extracted with methanol/chloroform (1:1) for 24 hours. The 4-OHE_2-1-N3Ade and 4-OHE_2-1-N7Gua were then separated by HPLC according to the references of 4-OHE_2-1-N3Ade and 4-OHE_2-1-N7Gua. The purified adducts were subjected to a Q-TOF mass spectrometry with following parameter: autosampler temperature, 4 °C; injection volume: 4 μl; ESI mode and voltage: 4000 V (+) ion mode; pump solvent: 50% methanol and 50% acetonitrile; flow rate: 0.5 ml/min. Data was acquired at a rate of 2.5 spectra/s with a stored mass range of m/z 50–1500. Data was collected and analyzed using Agilent MassHunter Workstation Data software. The peak values of 4-OHE_2-1-N3Ade and 4-OHE_2-1-N7Gua

showed the relative abundance of these adducts derived from different samples. Unmodified adenine or guanine was used as the loading control.

Detection of CE_2

Extraction of CE_2 (4-OHE_2 and 2-OHE_2) was performed according to the previous study with minor revision. In brief, approximately 1 g of ground mammary tissue was suspended in 2 ml of 50 mM ammonium acetate (pH 5.0) followed by addition of methanol with the final concentration of 60%. The mixture was extracted with 4 ml hexane to remove lipids. The aqueous phase was then diluted to an approximate final concentration of 25 % methanol with 30 mM ammonium acetate buffer, pH 4.4, containing 2 mg/ml ascorbic acid (to minimized oxidation of CE). The resulting solution was filtered through a 10 kDa MWCO ultrafilter to reduced protein interference and turbidity. Sample was immediately run on HPLC and the Q-TOF mass spectrometry with the following parameter: autosampler temperature, 4 °C; injection volume: 2 μl; ESI mode and voltage: 4000 V (−) ion mode; pump solvent: 50% methanol and 50% acetonitrile; flow rate: 0.5 ml/min. Data was acquired at a rate of 2.5 spectra/s with a stored mass range of m/z 50–1500. Data was collected and analyzed using Agilent MassHunter Workstation Data software.

4-OHE_2 treatment of mice

WT and BBP female mice (10 weeks) were anesthetized with ether and subcutaneously injected with the same volume of DMSO or 4-OHE_2 solution under the nipple region of the fourth and fifth mammary glands on the single side. The dose of 4-OHE_2 was 100 nmol/gland in 20 μl of DMSO. After operation, mice were maintained and subjected for the indicated experiments.

Cell treatment

For 4-OHE_2 treatment, cells were cultured in the presence of 10 μM 4-OHE_2 or 4-OHE_2 with the indicated concentrations for 12 hours, and subjected to the following experiments. For 4-OHE_2 recovery experiment, cells were cultured in the presence of 10 μM 4-OHE_2 or 4-OHE_2 with the gradient concentrations (1, 5, and 10 μM) for 12 hours, and cultured in fresh medium for 24 hours followed by the further experiments. For tempol treatment, cells were incubated in the presence of 100 μM tempol or tempol with the gradient concentrations (10, 50, and 100 μM) during the culture.

Comet assay

Single-cell gel electrophoretic comet assay was performed under neutral conditions to detecting DSBs according to the previous study. Briefly, cells with or without the indicated treatment were recovered in normal culture medium for indicated time. Cells were collected and rinsed twice with ice-cold PBS; 2×10^4/ml cells were combined with 1 % LMAgarose at 40 °C at the ratio of 1:3 (v/v) and immediately pipetted onto slides. For cellular lysis, the slides were immersed in the neutral lysis solution (2 % sarkosyl, 0.5 M Na_2EDTA, 0.5 mg/ml proteinase K in pH 8.0) overnight at 37 °C in dark, followed by washing in the rinse buffer (90 mM Tris-HCl pH 8.5, 90 mM boric acid, 2mM Na_2EDTA) for 30 minutes with two repeats. Then, the slides were subjected to electrophoresis at 20 V (0.6 V/cm) for 25

minutes and stained in 2.5 μg/ml propidium iodide for 20 minutes. All images were taken with a fluorescence microscope and analyzed by Comet Assay IV software.

Tempol treatment

Tempol treatment was performed according to the previous reports. In brief, tempol was added in the drinking water (1 mM) of the female mice since their weaning, and the water bottles were changed weekly. The administration was continued till the sacrifice of the mice.

Statistical analyses

All experiments were performed in triplicates unless indicated otherwise. Means and standard deviations were plotted. Student's t-test was used for statistical analyses. The log-rank test was performed on the Kaplan-Meier survival curves.

Results

The BBP mice develop mammary gland tumors

BRCA1 mutation-induced breast cancer is always associated with p53 mutation. Since BRCA1 participates in DNA damage response and repair, loss of BRCA1 induces genomic instability and activates p53-depednent checkpoint, which suppresses cell growth. However, lacking p53 abolishes the checkpoint and induces the growth of transformed cells. Thus, mutations of BRCA1 frequently associate with p53 mutations during breast tumorigenesis(18). Since homozygous loss of p53 alone is sufficient to drive mammary tumorigenesis, we used heterozygous mice to promote BRCA1 null-induced mammary tumors, and generated *Blg-Cre*; $Brca1^{f/f}$; $p53^{f/+}$ mice (the BBP mice), in which the *Blg-Cre* allele drives Cre recombinase expression to conditionally knockout both alleles of *Brca1* and one allele of *p53* in mammary gland (Fig. S1A). The littermates *Blg-Cre*; $Brca1^{+/+}$; $p53^{+/+}$ mice were used for the control (the WT mice). All the parous BBP mice developed obvious mammary tumor (Fig. S1B and C). ~ 15 % of the mice even developed multiple mammary tumors (Fig. S1D). The average tumor free fraction of the BBP mice was 302 days (Fig. S1B). In agreement with previous report, histochemistry staining shows that these mammary tumors are invasive duct carcinomas with central necrosis (Fig. S1E), which resembles the features of human *BRCA1* deficiency breast tumor.

Oxidative damage in mammary gland

To study the molecular mechanism of mammary tumorigenesis, we ask if estrogen metabolites are mutagens to induce tumorigenesis. Estrogens (E_1: estrone; E_2: estradiol) are converted to catechol estrogens (CE), including 2- and 4-hydroxylated estrogens (2-, 4-OHE), by cytochromes P450. Under normal condition, 2-OHE and 4-OHE are O-methylated by catechol-O-methyltransferases for inactivation. However, if high level of estrogens generates excessive CE, the O-methylation inactivation could be incomplete. CE is then oxidized to semiquinones (CE-SQ) and further to CE-quinones (CE-Q) including E-2,3-Q and E-3,4-Q. E-3,4-Q is a type of dangerous ROS, which attacks genomic DNA to form depurinating adducts including 4-OHE-1-N7Gua and 4-OHE-1-N3Ade (Fig. 1A) (19,20).

To examine this possibility in vivo, we harvested mammary glands from parous mice at the age of 25 weeks. Using mass spectrometry, we examined endogenous DNA adducts and found 4-OHE_2-1-N3Ade and 4-OHE_2-1-N7Gua as the molecular weight of these adducts is identical to standard references (Fig. 1B). However, these adducts were extremely difficult to be detected in the virgin mice (Fig. 1B). We also examined the level of metabolizes of estrogens. Since CE-SQ and CE-Q are short-live free radicals (21), it is unlikely to be detected by mass spectrometry. However, CE_2 was easily found in the mammary tissue extracts from the parous mice (Fig. 1C), suggesting that excessive CE_2 is like to induce estrogen-DNA adducts.

Since the depurinating adducts directly generate AP sites, we examined AP sites in vivo. Although few AP sites positive cells were found in the mammary glands from the virgin WT and BBP mice, a large amount of AP sites positive cells were identified in the mammary glands from the parous mice (Fig. 1D, Fig. S2A). Usually, AP sites are repaired by base excision repair (BER) machinery. However, if too many AP sites occurs simultaneously, some lesions may not be repaired timely, which can be converted into DSBs (22). Thus, we also examined DSBs in mammary tissues using γH2AX as a surrogate marker. Interestingly, cells with DSBs were only existed in the mammary gland isolated from the parous BBP but not from the WT or virgin BBP mice (Fig. 1E, Fig. S2B), suggesting that cells lacking Brca1 fail to repair DSBs induced by oxidized estrogens.

4-OHE_2 induces depurinating DNA adducts and DSBs *in vitro*

To validate the *in vivo* results, HCC1937, a human breast cancer cell line lacking BRCA1, was treated with or without 4-OHE_2. Both 4-OHE_2-1-N3Ade and 4-OHE_2-1-N7Gua were identified in the HCC1937 cell lysates (Fig. 2A). Similar results were obtained from HCC1937 cells reconstituted with wild type BRCA1 (HCC1937 BRCA1). Moreover, following 4-OHE_2 treatment, AP sites were detected in both HCC1937 and HCC1937 BRCA1 cells (Fig. 2B). Since unrepaired AP sites could be converted into DSBs, we also examined DSBs induced by 4-OHE_2 treatment by γH2AX staining. Indeed, 4-OHE_2 treatment caused DSBs in HCC1937 and HCC1937 BRCA1 cells (Fig. 2C). Interestingly, after recovery for 24 hours, DSBs were repaired in HCC1937 BRCA1 cells but not in HCC1937 cells (Fig. 2C). These results were further confirmed by neutral comet assays as 4-OHE_2-induced DSBs were clearly observed in HCC1937 cells but quickly repaired in HCC1937 BRCA1 cells (Fig. 2D). Collectively, these results suggest that excessive estrogen induces oxidative damage on genomic DNA, such as AP sites. If AP sites are too many to be timely repaired, the AP sites could be converted into DSBs. With BRCA1, DSBs are quickly repaired for genomic stability. However, lacking of BRCA1, DSBs are difficult to be repaired, which may induce genomic instability and tumorigenesis.

To further examine the defects of DSB repair in BRCA1 deficient cells, we examined the downstream effectors of BRCA1. It has been shown that BRCA1 is required for CHK1 activation in response to DSBs. Since Ser345 phosphorylation is a surrogate maker of CHK1 activation, we treated HCC1937 and HCC1937 BRCA1 cells with 4-OHE_2. Activated CHK1 was observed in HCC1937 BRCA1 cells, while the active CHK1 in HCC1937 cells was much impaired (Fig. S3). Moreover, BRCA1 is required for loading RAD51, the key HR

recombinase for DSB repair. Thus, in 4-OHE_2-treated HCC1937 BRCA1 cells, RAD51 is recruited to the sites of DSBs (Fig. S4). However, DSB-induced RAD51 foci formation was impaired in HCC1937 cells (Fig. S4). Taken together, these results suggest that estrogen metabolites-induced DSB response is impaired in BRCA1-deficient cells.

4-OHE_2 induces DNA damage and mammary tumorigenesis *in vivo*

To examine the role of estrogen metabolites in tumorigenesis in vivo, Parous mice at the age of 14 weeks were treated with 4-OHE_2 via subcutaneous injection surrounding nipple area. A significant amount of 4-OHE_2-1-N3Ade and 4-OHE_2-1-N7Gua were found in mammary glands in both WT and BBP mice (Fig. 3A). Consistently, AP sites were identified in mammary glands treated with 4-OHE_2 (Fig. 3B). Since a large number of AP sites may induce DSBs, we also examined DSBs in 4-OHE_2-treated mammary glands with γH2AX staining. Although cells with positive γH2AX staining were identified in both WT and BBP mice (Fig. 3C), the level of γH2AX in the BBP mice was much higher than that in the WT mice (Fig. 3D). It suggests that following 4-OHE_2 treatment, unrepaired DSBs in the WT mice were much less than those in the BBP mice. Since unrepaired DSBs cause genomic instability and tumorigenesis, we monitored mammary tumorigenesis in 4-OHE_2-treated mice. Correlated with 4-OHE_2-induced DSBs, 4-OHE_2 treatment shortens the latency of mammary gland tumors in the BBP mice. (Fig. 3E). In addition, 4-OHE_2 injection was also injected into the virgin mice at 10-week old, which also accelerate the onset of mammary gland tumors in these mice (Fig. S5). Collectively, these results suggest that 4-OHE_2 treatment induces DNA lesions, such as DSBs, in vivo. Lacking BRCA1, unrepaired DSBs are likely to induce tumorigenesis in mammary gland.

Antioxidant treatment suppresses estrogen-induced DNA damage and mammary tumorigenesis

Since estrogen metabolites induce DNA damage and genomic instability in mammary gland, we ask if antioxidant treatment could suppress estrogen-induced DNA damage. Accumulated evidence has shown that tempol (4-hydroxy-2,2,6,6-tetramethylpiperidine-N-oxyl) is a potent free radical scavenger both in vitro and in vivo (23,24). Thus, we pretreated HCC1937 and HCC1937 BRCA1 cells with tempol before exposure to 4-OHE_2. We found that the level of 4-OHE_2-1-N3Ade and 4-OHE_2-1-N7Gua were significantly reduced (Fig. 4A). Moreover, tempol treatment suppressed the 4-OHE_2-induced AP sites and DSBs in HCC1937 cells (Fig. 4B and C). In particular, neutral comet assays showed that 4-OHE_2-induced DSBs were suppressed by tempol in a dose-dependent manner (Fig. 4D). Taken together, it suggests that tempol treatment effectively suppresses free radical generation during estrogen metabolism.

Next, we ask if tempol treatment regulates estrogen-induced DNA damage in vivo and mammary tumorigenesis in the BBP mice. 1 mM tempol was supplemented in the drinking water after weaning of the BBP mice at the age of three weeks. Again, endogenous level of 4-OHE_2-1-N3Ade and 4-OHE_2-1-N7Gua were significantly reduced in the mammary gland of the parous BBP mice (Fig. 5A). Next, we examined and found that both AP sites and DSBs were suppressed following tempol treatment in the mammary glands of parous mice (Fig. 5B and C). More importantly, tempol treatment significantly delayed the onset of

mammary tumorigenesis in the BBP mice (Fig. 5D). Thus, these results suggest that antioxidant treatment could be an important chemoprevention approach for suppressing BRCA1-deficient tumor in vivo.

Discussion

In this study, we demonstrate that oxidized estrogen is a critical carcinogen to induce DNA damage and mammary tumors in *BRCA1*-deficient mice. Tempol treatment suppresses estrogen-induced DNA damage and mammary tumorigenesis. Accumulated evidence shows that BRCA1 plays an important role in DSB repair (25,26). Mutation of BRCA1 abolishes DNA damage repair and induces genomic instability (27). Thus, BRCA1 should be an important tumor suppressor for many types of cancers. However, mutation of BRCA1 mainly induces breast and ovarian cancers (28,29). Here, we show that oxidized estrogen causes numerous AP sites in vivo. Although most AP sites are quickly repaired by BER, a small set of unrepaired AP sites could be converted to DSBs during DNA replication or two AP sites are close to each other. Thus, we observed oxidized estrogen-induced DSBs both in vitro and in vivo. Once DSBs occur, these lesions have to be error-free repaired. Otherwise, these lesions will directly cause genomic instability (30). BRCA1 has been shown to play a key role in HR, the major type error-free repair for DSBs (31–33). Thus, without BRCA1, cells could not repair DSBs and are transformed to tumor cells. Moreover, since estrogens are mainly generated in ovary and breast tissues, excessive estrogen-induced DNA damage occurs in breast and ovary (34–36). Lacking BRCA1, cells could not timely repair estrogen-induced DNA damage in breast and ovary, which cause genomic instability and tumorigenesis in these tissues. Consistently, mutations of other DSB repair machineries are also observed in breast and ovarian cancer (37), suggesting that DSB repair plays a key role to protect genomic integrity and suppresses breast and ovarian tumorigenesis.

In addition, one important clinical feature for BRCA1 mutation-induced breast cancer is the early onset of the tumor as many patients develop breast cancer before the age of 40 (38–40). Since it may take decades for a few transformed cells (or tumor stem cells) to grow into a tumor mass, it is likely that breast tissue-specific DNA damage occurs in the early age of breast cancer patients. Estrogen reaches the highest level to promote ductal development from puberty to pregnancy (41). The high level of estrogen generates ROS to induce DNA damage. Lacking of BRCA1 allows the accumulation of DNA lesions without repair, which induces genomic instability and tumorigenesis. Thus, excessive estrogen could be a non-genetic force to induce genomic instability and breast tumorigenesis. To support this notion, it has been shown that both pregnancy and estrogen supplement are associated with an increased breast cancer risk for BRCA1 mutation carrier (42–44). One function of estrogen is to induce ductal development in mammary gland. During the ductal development, it is the luminal progenitor cells that receive estrogen and differentiate into luminal epithelial cells. And it has been shown that the luminal progenitor is the origin for basal-like breast cancers arising in BRCA1 mutation carriers. Thus, it is likely that the high level of estrogen causes DNA damage and induces genomic instability in the luminal progenitors, and induces tumorigenesis in the absence of BRCA1. In contrast, the cell origin of luminal breast cancer remains elusive. In particular, the profile of luminal A suggests that it might originate from progenitor cells close to mature luminal cells. Thus, it is likely that other mechanism induces

luminal cell transformation and causes luminal breast cancer. Due to technical limitation, we could not specifically delete Brca1 in luminal projector. Instead, we used beta-lactoglobulin (Blg) cre to genetically remove Brca1 in mammary tissue during the mammary gland development. In addition, we have not found any link between the ER expression and the oxidative metabolites of estrogen. It has been shown that BRCA1 might facilitate the expression of ERα (45). Thus, it is possible that lacking BRCA1 may reduce the expression of ERα, and indirectly accumulate estrogen or estrogen metabolites. But further study is needed to test the hypothesis. Taken together, our study may address the question why BRCA1 mutation only induces tissue-specific cancers.

Our study also shows that antioxidant treatment suppresses estrogen-induced DNA lesions and mammary tumorigenesis, indicating that antioxidant could be used in the chemoprevention for BRCA1 mutation-induced breast cancer. BRCA1 mutation-induced breast cancer has an aggressive phenotype similar to the estrogen receptor negative, progesterone receptor negative and HER2 negative breast cancer (46–48). However, personalized medicine for familial breast cancer has not been developed. Despite the advance on killing cancer cells with general radiotherapy and chemotherapy, these approaches cannot avoid the side effects that affect the life quality of cancer patients (49). Thus, antioxidant supplemental could be a novel approach for the eradication of familial breast cancer. In our study, tempol treatment significantly delayed the onset of mammary tumorigenesis in the BBP mice, but did not eradicate the mammary tumorigenesis. It is because one allele of *p53* has been deleted by Cre recombinase in mammary tissues. Heterozygosity of *p53* alone is sufficient to induce genomic instability and mammary tumorigenesis although with long latency(50).

We also realize that high level of estrogen exists in every pregnant woman. However, with robust BER capacity, cells are likely to repair most AP sites induced by oxidized estrogen. In the presence of BRCA1, cells are able to repair the remaining DSBs converted from unrepaired AP sites. Thus, endogenous high level of estrogen does not induce genomic instability and mammary tumorigenesis when cells are equipped with intact DNA repair machinery. However, long term estrogen supplement is indeed associated with an increased breast cancer risk even for women without BRCA1 mutation. Thus, when exposed to high level of exogenous estrogen, people who carry the mutations in DNA repair system should be very cautious.

Supplementary Material

Refer to Web version on PubMed Central for supplementary material.

Acknowledgments

Financial Disclosure: This work was supported by grants from National Institutes of Health, CA132755, CA130899 and CA187209 to X. Yu. National Natural Science Foundation of China (No. 81672610) to M. Li. X. Yu is a recipient of Era of Hope Scholar Award from the Department of Defense. M. Li is supported by Ovarian Cancer Research Fund.

We thank Dr. Kathleen Cho and Dr. Yuan Zhu for providing the *BRCA1*$^{flox/+}$ mice and *p53*$^{flox/+}$ mice, respectively.

References

1. Friedman LS, Ostermeyer EA, Szabo CI, Dowd P, Lynch ED, Rowell SE, et al. Confirmation of BRCA1 by analysis of germline mutations linked to breast and ovarian cancer in ten families. Nat Genet. 1994; 8:399–404. [PubMed: 7894493]
2. Miki Y, Swensen J, Shattuck-Eidens D, Futreal PA, Harshman K, Tavtigian S, et al. A strong candidate for the breast and ovarian cancer susceptibility gene BRCA1. Science. 1994; 266:66–71. [PubMed: 7545954]
3. Esteller M, Silva JM, Dominguez G, Bonilla F, Matias-Guiu X, Lerma E, et al. Promoter hypermethylation and BRCA1 inactivation in sporadic breast and ovarian tumors. J Natl Cancer Inst. 2000; 92:564–9. [PubMed: 10749912]
4. Li ML, Greenberg RA. Links between genome integrity and BRCA1 tumor suppression. Trends Biochem Sci. 2012; 37:418–24. [PubMed: 22836122]
5. Cortez D, Wang Y, Qin J, Elledge SJ. Requirement of ATM-dependent phosphorylation of brca1 in the DNA damage response to double-strand breaks. Science. 1999; 286:1162–6. [PubMed: 10550055]
6. Tibbetts RS, Cortez D, Brumbaugh KM, Scully R, Livingston D, Elledge SJ, et al. Functional interactions between BRCA1 and the checkpoint kinase ATR during genotoxic stress. Genes Dev. 2000; 14:2989–3002. [PubMed: 11114888]
7. Chen J. Ataxia telangiectasia-related protein is involved in the phosphorylation of BRCA1 following deoxyribonucleic acid damage. Cancer Res. 2000; 60:5037–9. [PubMed: 11016625]
8. Abraham RT. Cell cycle checkpoint signaling through the ATM and ATR kinases. Genes Dev. 2001; 15:2177–96. [PubMed: 11544175]
9. Scully R, Chen J, Plug A, Xiao Y, Weaver D, Feunteun J, et al. Association of BRCA1 with Rad51 in mitotic and meiotic cells. Cell. 1997; 88:265–75. [PubMed: 9008167]
10. Xia B, Sheng Q, Nakanishi K, Ohashi A, Wu J, Christ N, et al. Control of BRCA2 cellular and clinical functions by a nuclear partner, PALB2. Mol Cell. 2006; 22:719–29. [PubMed: 16793542]
11. Moynahan ME, Chiu JW, Koller BH, Jasin M. Brca1 controls homology-directed DNA repair. Mol Cell. 1999; 4:511–8. [PubMed: 10549283]
12. Xu X, Qiao W, Linke SP, Cao L, Li WM, Furth PA, et al. Genetic interactions between tumor suppressors Brca1 and p53 in apoptosis, cell cycle and tumorigenesis. Nat Genet. 2001; 28:266–71. [PubMed: 11431698]
13. Molyneux G, Geyer FC, Magnay FA, McCarthy A, Kendrick H, Natrajan R, et al. BRCA1 basal-like breast cancers originate from luminal epithelial progenitors and not from basal stem cells. Cell Stem Cell. 2010; 7:403–17. [PubMed: 20804975]
14. Clemons M, Goss P. Estrogen and the risk of breast cancer. N Engl J Med. 2001; 344:276–85. [PubMed: 11172156]
15. Li KM, Todorovic R, Devanesan P, Higginbotham S, Kofeler H, Ramanathan R, et al. Metabolism and DNA binding studies of 4-hydroxyestradiol and estradiol-3,4-quinone in vitro and in female ACI rat mammary gland in vivo. Carcinogenesis. 2004; 25:289–97. [PubMed: 14578156]
16. Savage KI, Matchett KB, Barros EM, Cooper KM, Irwin GW, Gorski JJ, et al. BRCA1 deficiency exacerbates estrogen-induced DNA damage and genomic instability. Cancer Res. 2014; 74:2773–84. [PubMed: 24638981]
17. Fuhrman BJ, Schairer C, Gail MH, Boyd-Morin J, Xu X, Sue LY, et al. Estrogen metabolism and risk of breast cancer in postmenopausal women. J Natl Cancer Inst. 2012; 104:326–39. [PubMed: 22232133]
18. Shakya R, Szabolcs M, McCarthy E, Ospina E, Basso K, Nandula S, et al. The basal-like mammary carcinomas induced by Brca1 or Bard1 inactivation implicate the BRCA1/BARD1 heterodimer in tumor suppression. Proc Natl Acad Sci U S A. 2008; 105:7040–5. [PubMed: 18443292]
19. Zahid M, Kohli E, Saeed M, Rogan E, Cavalieri E. The greater reactivity of estradiol-3,4-quinone vs estradiol-2,3-quinone with DNA in the formation of depurinating adducts: implications for tumor-initiating activity. Chem Res Toxicol. 2006; 19:164–72. [PubMed: 16411670]

20. Mannisto PT, Kaakkola S. Catechol-O-methyltransferase (COMT): biochemistry, molecular biology, pharmacology, and clinical efficacy of the new selective COMT inhibitors. Pharmacol Rev. 1999; 51:593–628. [PubMed: 10581325]
21. Hachey DL, Dawling S, Roodi N, Parl FF. Sequential action of phase I and II enzymes cytochrome p450 1B1 and glutathione S-transferase P1 in mammary estrogen metabolism. Cancer Res. 2003; 63:8492–9. [PubMed: 14679015]
22. Jackson SP, Bartek J. The DNA-damage response in human biology and disease. Nature. 2009; 461:1071–8. [PubMed: 19847258]
23. Schubert R, Erker L, Barlow C, Yakushiji H, Larson D, Russo A, et al. Cancer chemoprevention by the antioxidant tempol in Atm-deficient mice. Hum Mol Genet. 2004; 13:1793–802. [PubMed: 15213104]
24. Yamada J, Yoshimura S, Yamakawa H, Sawada M, Nakagawa M, Hara S, et al. Cell permeable ROS scavengers, Tiron and Tempol, rescue PC12 cell death caused by pyrogallol or hypoxia/reoxygenation. Neurosci Res. 2003; 45:1–8. [PubMed: 12507718]
25. Sy SM, Huen MS, Chen J. PALB2 is an integral component of the BRCA complex required for homologous recombination repair. Proc Natl Acad Sci U S A. 2009; 106:7155–60. [PubMed: 19369211]
26. Khanna KK, Jackson SP. DNA double-strand breaks: signaling, repair and the cancer connection. Nat Genet. 2001; 27:247–54. [PubMed: 11242102]
27. Venkitaraman AR. Cancer susceptibility and the functions of BRCA1 and BRCA2. Cell. 2002; 108:171–82. [PubMed: 11832208]
28. Rahman N, Stratton MR. The genetics of breast cancer susceptibility. Annu Rev Genet. 1998; 32:95–121. [PubMed: 9928476]
29. Easton DF, Ford D, Bishop DT. Breast and ovarian cancer incidence in BRCA1-mutation carriers. Breast Cancer Linkage Consortium. Am J Hum Genet. 1995; 56:265–71. [PubMed: 7825587]
30. van Gent DC, Hoeijmakers JH, Kanaar R. Chromosomal stability and the DNA double-stranded break connection. Nat Rev Genet. 2001; 2:196–206. [PubMed: 11256071]
31. Zhang F, Ma J, Wu J, Ye L, Cai H, Xia B, et al. PALB2 links BRCA1 and BRCA2 in the DNA-damage response. Curr Biol. 2009; 19:524–9. [PubMed: 19268590]
32. West SC. Molecular views of recombination proteins and their control. Nat Rev Mol Cell Biol. 2003; 4:435–45. [PubMed: 12778123]
33. Hoeijmakers JH. Genome maintenance mechanisms for preventing cancer. Nature. 2001; 411:366–74. [PubMed: 11357144]
34. Cunat S, Hoffmann P, Pujol P. Estrogens and epithelial ovarian cancer. Gynecol Oncol. 2004; 94:25–32. [PubMed: 15262115]
35. Clinton GM, Hua W. Estrogen action in human ovarian cancer. Crit Rev Oncol Hematol. 1997; 25:1–9. [PubMed: 9134308]
36. Ho SM. Estrogen, progesterone and epithelial ovarian cancer. Reprod Biol Endocrinol. 2003; 1:73. [PubMed: 14577831]
37. Lord CJ, Ashworth A. The DNA damage response and cancer therapy. Nature. 2012; 481:287–94. [PubMed: 22258607]
38. King MC, Marks JH, Mandell JB. Breast and ovarian cancer risks due to inherited mutations in BRCA1 and BRCA2. Science. 2003; 302:643–6. [PubMed: 14576434]
39. Offit K, Gilewski T, McGuire P, Schluger A, Hampel H, Brown K, et al. Germline BRCA1 185delAG mutations in Jewish women with breast cancer. Lancet. 1996; 347:1643–5. [PubMed: 8642955]
40. Peto J, Collins N, Barfoot R, Seal S, Warren W, Rahman N, et al. Prevalence of BRCA1 and BRCA2 gene mutations in patients with early-onset breast cancer. J Natl Cancer Inst. 1999; 91:943–9. [PubMed: 10359546]
41. De Hertogh R, Thomas K, Bietlot Y, Vanderheyden I, Ferin J. Plasma levels of unconjugated estrone, estradiol and estriol and of HCS throughout pregnancy in normal women. J Clin Endocrinol Metab. 1975; 40:93–101. [PubMed: 1112883]

42. Marsden J. Hormone-replacement therapy and breast cancer. Lancet Oncol. 2002; 3:303–11. [PubMed: 12067808]
43. Cullinane CA, Lubinski J, Neuhausen SL, Ghadirian P, Lynch HT, Isaacs C, et al. Effect of pregnancy as a risk factor for breast cancer in BRCA1/BRCA2 mutation carriers. Int J Cancer. 2005; 117:988–91. [PubMed: 15986445]
44. Hilakivi-Clarke L. Estrogens, BRCA1, and breast cancer. Cancer Res. 2000; 60:4993–5001. [PubMed: 11016617]
45. Hosey AM, Gorski JJ, Murray MM, Quinn JE, Chung WY, Stewart GE, et al. Molecular basis for estrogen receptor alpha deficiency in BRCA1-linked breast cancer. J Natl Cancer Inst. 2007; 99:1683–94. [PubMed: 18000219]
46. Foulkes WD, Smith IE, Reis-Filho JS. Triple-negative breast cancer. N Engl J Med. 2010; 363:1938–48. [PubMed: 21067385]
47. Young SR, Pilarski RT, Donenberg T, Shapiro C, Hammond LS, Miller J, et al. The prevalence of BRCA1 mutations among young women with triple-negative breast cancer. BMC Cancer. 2009; 9:86. [PubMed: 19298662]
48. Cleator S, Heller W, Coombes RC. Triple-negative breast cancer: therapeutic options. Lancet Oncol. 2007; 8:235–44. [PubMed: 17329194]
49. Partridge AH, Burstein HJ, Winer EP. Side effects of chemotherapy and combined chemohormonal therapy in women with early-stage breast cancer. J Natl Cancer Inst Monogr. 2001:135–42. [PubMed: 11773307]
50. Jonkers J, Meuwissen R, van der Gulden H, Peterse H, van der Valk M, Berns A. Synergistic tumor suppressor activity of BRCA2 and p53 in a conditional mouse model for breast cancer. Nat Genet. 2001; 29:418–25. [PubMed: 11694875]

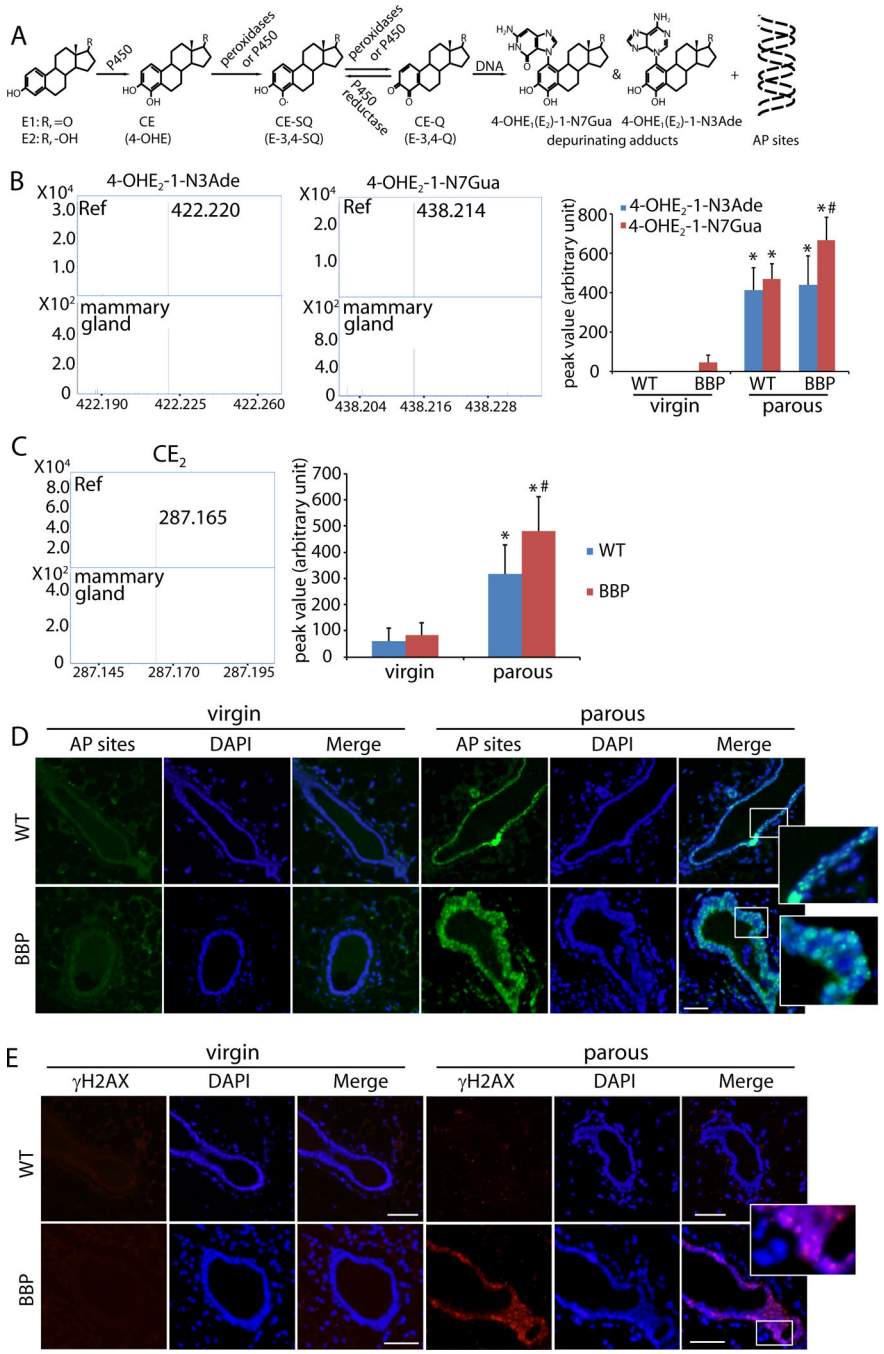

Figure 1. Estrogen oxidation-induced depurinating DNA adducts in mammary gland from parous mice

(A) Schematic diagram of generation of estrogen oxidative metabolites and estrogen oxidation-induced depurinating DNA adducts *in vivo*. (B) Depurinating DNA adducts in mammary gland are detected by LC-MS. Chemical synthesized 4-OHE_2-1-N3Ade and 4-OHE_2-1-N7Gua (Ref) are shown with the molecular weight of 422.220 and 438.124, respectively; 4-OHE_2-1-N3Ade and 4-OHE_2-1-N7Gua derived from precancerous mammary gland of parous BBP mice (25 weeks) were examined. Histogram shows the peak value from the Q-TOF mass spectrometry of 4-OHE_2-1-N3Ade and 4-OHE_2-1-N7Gua in mammary

glands from virgin (10 weeks) or parous mice (25 weeks). Mammary glands from both WT and BBP mice were examined. (C) CE_2 (4-OHE_2 and 2-OHE_2) in mammary gland was detected by Q-TOF mass spectra. Commercial reference of 4-OHE_2 with the molecular weight of 287.165 (ref); CE_2 derived from precancerous mammary gland of parous BBP mice (mammary gland). Histogram shows the relative level of CE_2 in WT and precancerous BBP mammary gland from virgin or parous mice. * and #, $p < 0.01$, respectively. (D) AP sites staining in mammary glands from the WT and BBP mice (25 weeks). (E) Immunostaining of γH2AX in mammary glands from the WT and BBP mice (25 weeks). Scale bars: 50 μm.

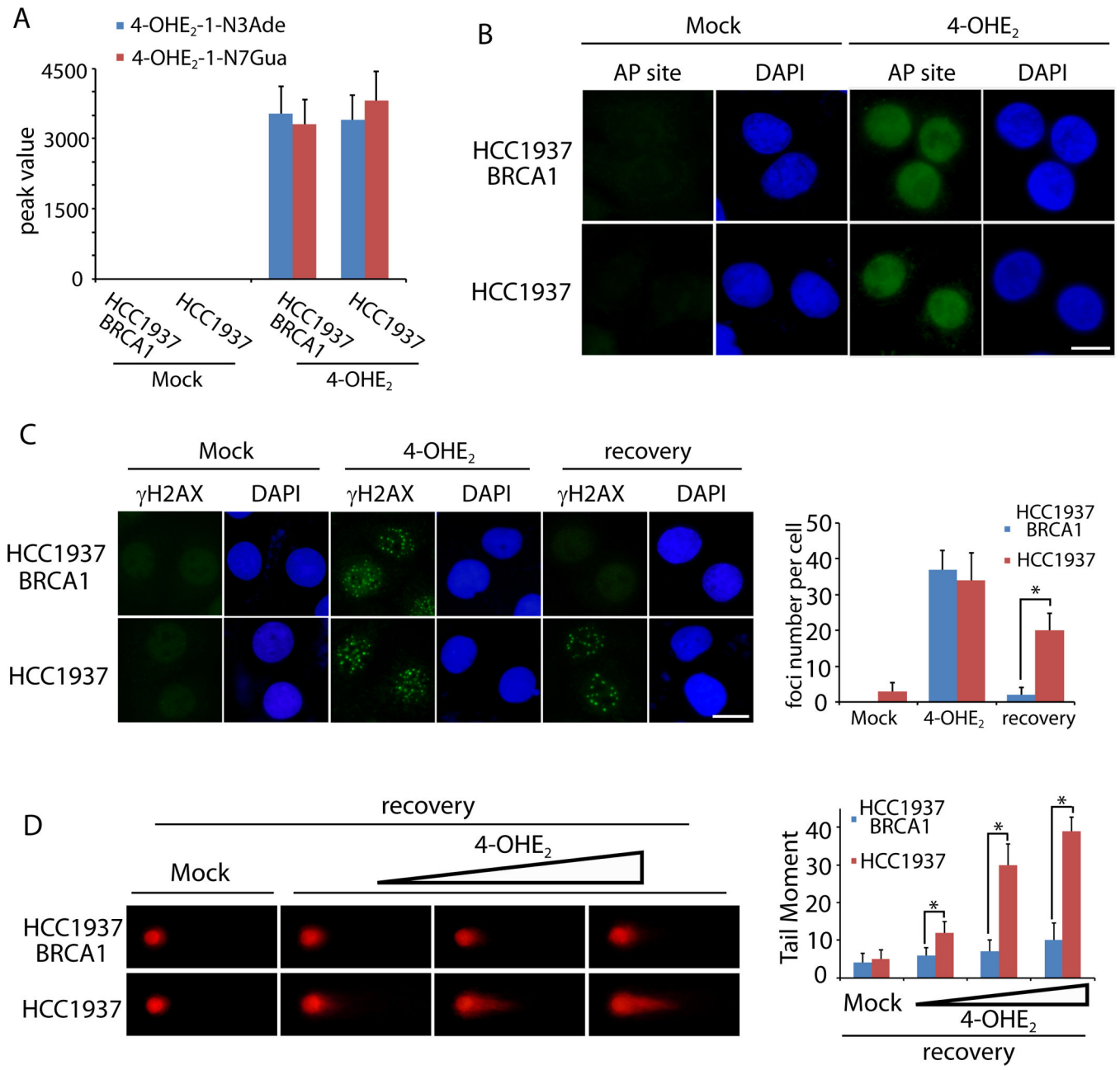

Figure 2. 4-OHE$_2$ induces DNA lesions *in vitro*

(A) 4-OHE$_2$ treatment induces depurinating DNA adducts in cells. HCC1937 BRCA1 and HCC1937 cells were treated with or without 4-OHE$_2$. Peak values of cellular 4-OHE$_2$-1-N3Ade and 4-OHE$_2$-1-N7Gua in mass spectrometry are shown. (B) 4-OHE$_2$ treatment induces AP sites in cells. HCC1937 BRCA1 and HCC1937 cells were treated with mock or 10 μM 4-OHE$_2$ for 12 hours followed by AP sites staining. (C) Immunostaining of γH2AX in cells. HCC1937 BRCA1 and HCC1937 cells were treated with mock or 10 μM 4-OHE$_2$ for 12 hours followed by γH2AX staining. Alternatively, cells were recovered for 24 hours followed by γH2AX staining. Scale bars: 10 μm. Foci numbers from 50 cells were summarized in the histogram. *, $p < 0.01$. (D) 4-OHE$_2$-induced DSBs are examined by

neutral comet assay. HCC1937 BRCA1 and HCC1937 cells were treated with mock or 4-OHE_2 (1, 5, and 10 μM) for 12 hours followed by 2 hour recovery and neutral comet assay. Tail moment of the detected cells was summarized in the histogram. *, $p < 0.01$.

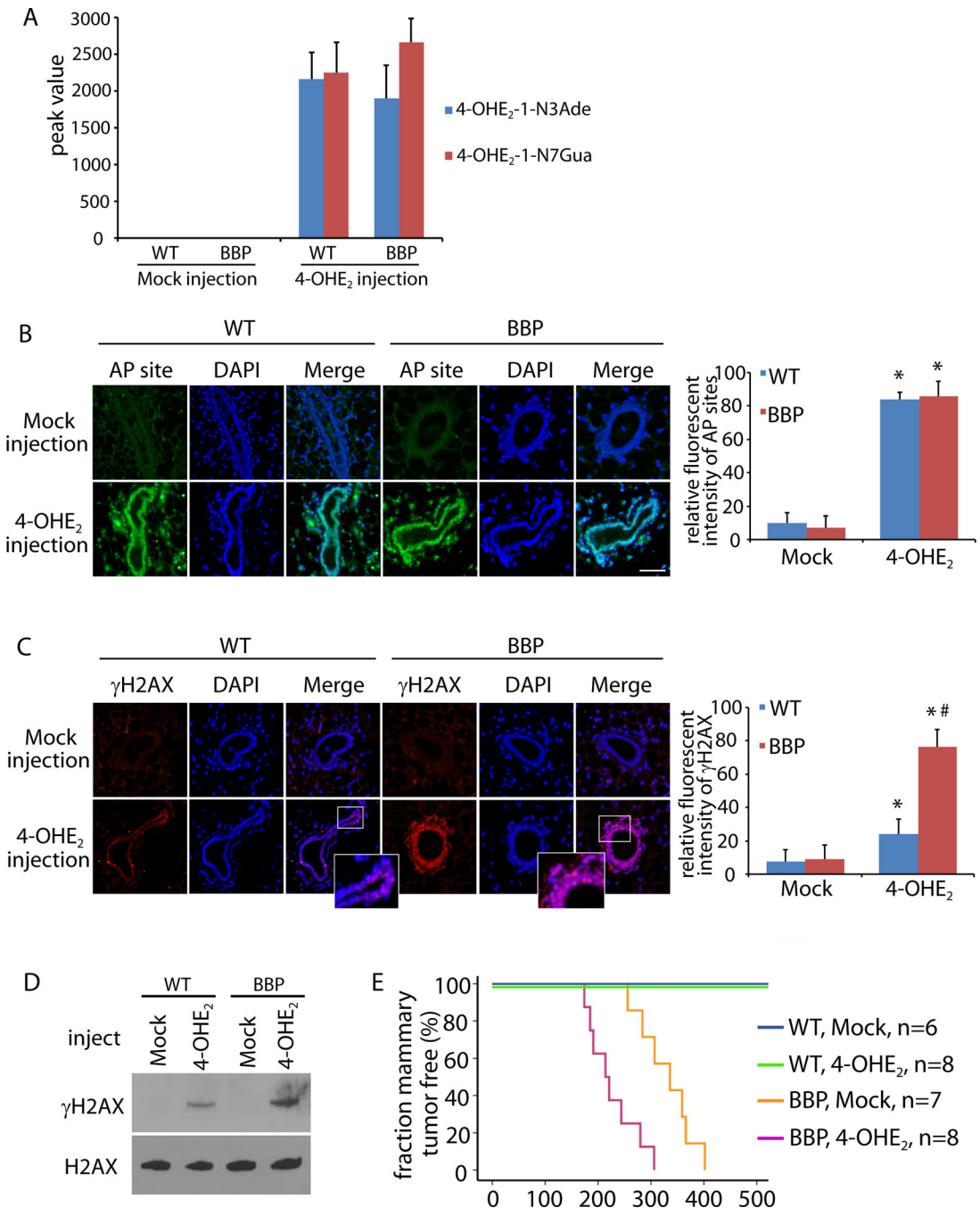

Figure 3. 4-OHE$_2$ injection induces DNA lesions and breast tumor *in vivo*

(A) 4-OHE$_2$ injection induces 4-OHE$_2$-1-N3Ade and 4-OHE$_2$-1-N7Gua in mammary gland. Peak values of 4-OHE$_2$-1-N3Ade and 4-OHE$_2$-1-N7Gua from mammary gland of parous WT and BBP mice (10 weeks) in mass spectrometry are shown. (B, C) 4-OHE$_2$ injection induces AP sites (B) and DSBs (C) in mammary gland of WT and BBP parous mice (14 weeks). Scale bars: 50 μm. Fluorescent intensity of AP sites (B) and γH2AX (C) was analyzed by Image J software. * and #, $p < 0.01$, respectively. (D) Phosphorylation of H2AX in mammary tissues from the injected WT and BBP mice was detected by Western blot.

Total H2AX was used as the loading control. (E) Kaplan-Meier analysis shows the mammary tumor free fraction of WT and BBP mice injected with mock or 4-OHE_2. The medians of tumor free BBP mice injected with mock or 4-OHE_2 are 335 and 214 day, respectively.

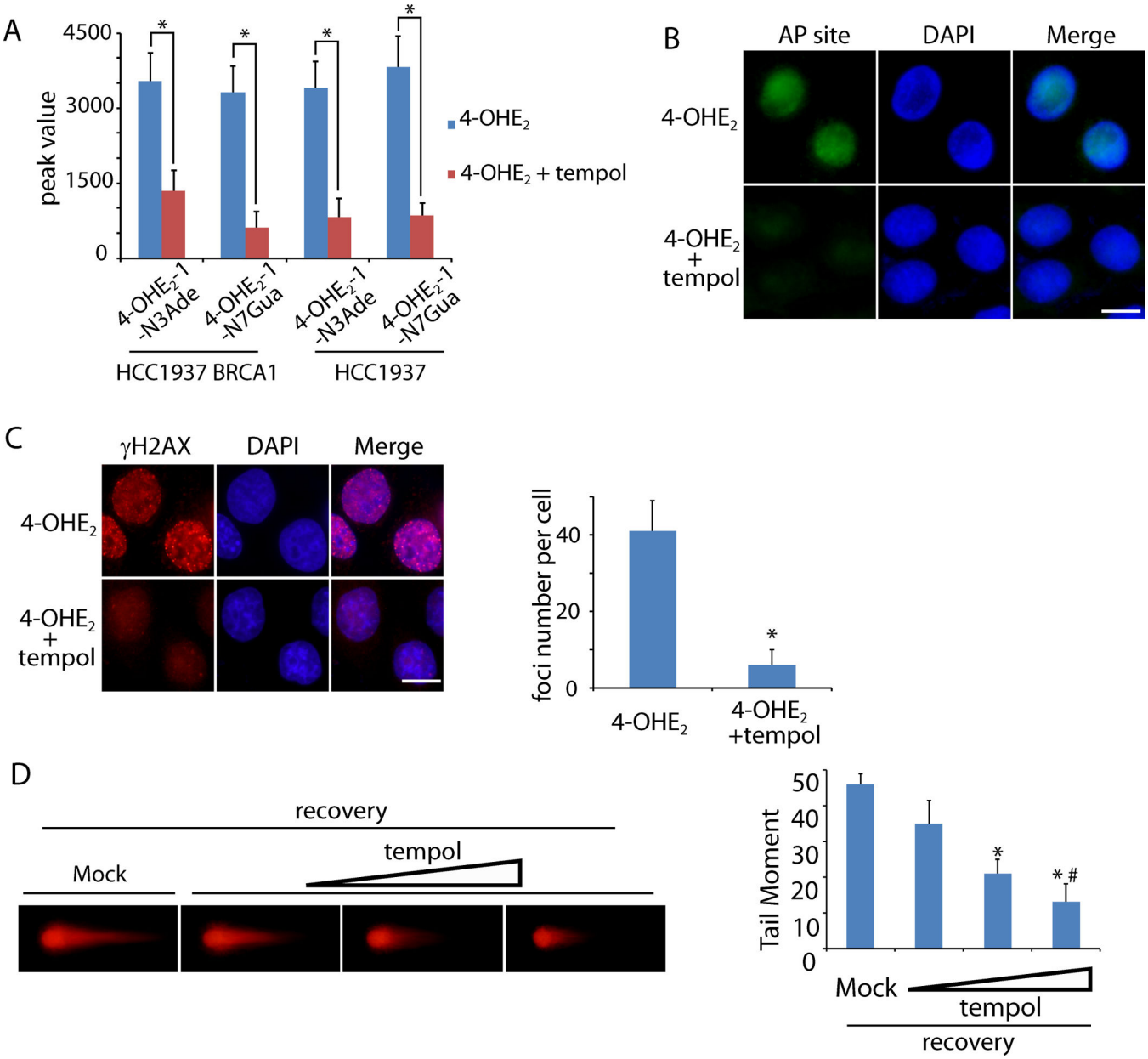

Figure 4. Tempol treatment suppresses 4-OHE$_2$-induced DNA lesions *in vitro*

(A) Tempol treatment suppresses 4-OHE$_2$-1-N3Ade and 4-OHE$_2$-1-N7Gua. HCC1937 BRCA1 and HCC1937 cells were preincubated with mock or tempol followed by the treatment of 4-OHE$_2$. The levels of 4-OHE$_2$-1-N3Ade and 4-OHE$_2$-1-N7Gua were examined by mass spectrometry. (B) AP sites are remarkably reduced in the presence of tempol. HCC1937 cells were preincubated with or without tempol followed by the treatment of 4-OHE$_2$. (C, D) Tempol treatment suppresses 4-OHE$_2$-induced DSBs. (C) Foci of γH2AX in HCC1937 cells were examined. Scale bars: 10 μm. Foci numbers of γH2AX in each cell are shown in the graph. (D) HCC1937 cells were preincubated with mock or tempol (20, 50, and 100 μM). Neutral comet assays were performed to examine 4-OHE$_2$-

induced DSBs. Tail moments of the cells treated with different doses of tempol are shown in the histogram. * and #, $p < 0.01$, respectively.

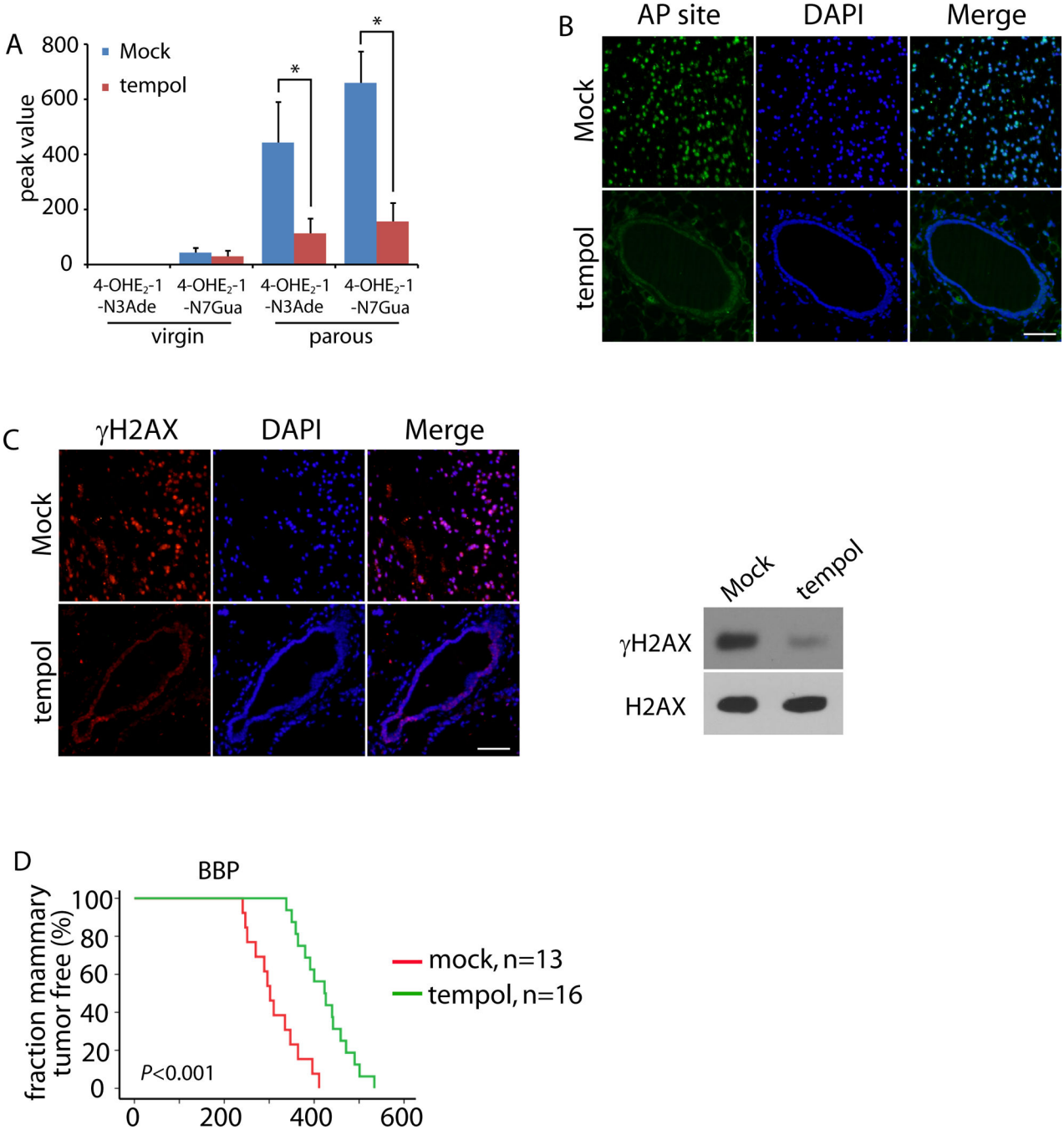

Figure 5. Tempol treatment suppresses 4-OHE$_2$-induced DNA damage *in vivo* and delays the breast tumor onset in parous BBP mice

(A) Tempol decreases the DNA adducts in mammary gland of parous BBP mice. The levels of 4-OHE$_2$-1-N3Ade and 4-OHE$_2$-1-N7Gua in mammary gland of the virgin and parous BBP mice (25 weeks) treated with or without tempol were examined by mass spectrometry. *, $p < 0.01$. (B, C) Tempol treatment suppresses AP sites (B) and DSBs (C) in the mammary glands of parous BBP mice (40 weeks). Immunostaining of γH2AX indicates DSBs. Scale bar: 50 μm. (D) Kaplan-Meier analysis of the mammary tumor free fraction of parous BBP

mice treated with mock or tempol. The median tumor free fractions are 302 and 423 days, respectively.